B.1.617.2 enters and fuses lung cells with increased efficiency and evades antibodies induced by infection and vaccination

Graphical abstract
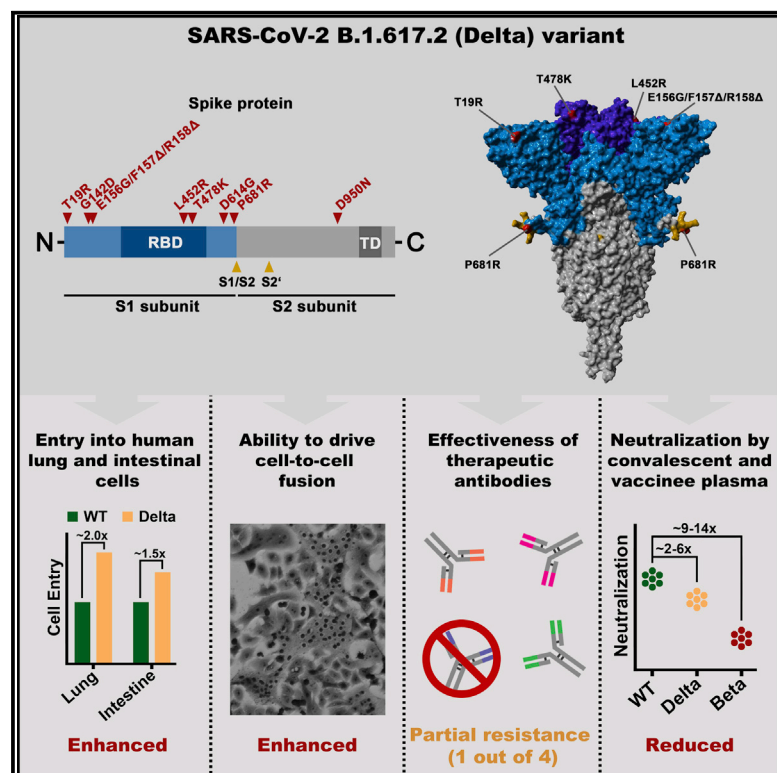
Authors

Prerna Arora, Anzhalika Sidarovich, Nadine Krüger, ..., Georg M.N. Behrens, Stefan Pöhlmann, Markus Hoffmann

Correspondence

spoehlmann@dpz.eu (S.P.), mhoffmann@dpz.eu (M.H.)

In brief

The B.1.617.2 (Delta) variant challenges efforts to control the COVID-19 pandemic. Arora et al. provide evidence that B.1.617.2 may enter human lung cells and fuse neighboring cells more efficiently than the initially circulating virus. Further, the study suggests that B.1.617.2 may evade neutralization by antibodies elicited upon infection and vaccination.

Highlights

- B.1.617.2 spike mediates enhanced entry into Calu-3 and Caco-2 cells

- B.1.617.2 spike fuses cells more efficiently than wild-type spike

- B.1.617.2 spike is bamlanivimab resistant

- B.1.617.2 spike evades neutralizing antibodies induced by infection or vaccination

Report

B.1.617.2 enters and fuses lung cells with increased efficiency and evades antibodies induced by infection and vaccination

Prerna Arora,[1,2] Anzhalika Sidarovich,[1,2] Nadine Krüger,[1] Amy Kempf,[1,2] Inga Nehlmeier,[1] Luise Graichen,[1,2] Anna-Sophie Moldenhauer,[1] Martin S. Winkler,[3] Sebastian Schulz,[4] Hans-Martin Jäck,[4] Metodi V. Stankov,[5] Georg M.N. Behrens,[5] Stefan Pöhlmann,[1,2,6,*] and Markus Hoffmann[1,2,*]

[1]Infection Biology Unit, German Primate Center, Kellnerweg 4, 37077 Göttingen, Germany
[2]Faculty of Biology and Psychology, Georg-August-University Göttingen, Wilhelmsplatz 1, 37073 Göttingen, Germany
[3]Department of Anesthesiology, University of Göttingen Medical Center, Göttingen, Georg-August University of Göttingen, Robert-Koch-Straße 40, 37075 Göttingen, Germany
[4]Division of Molecular Immunology, Department of Internal Medicine 3, Friedrich-Alexander University of Erlangen-Nürnberg, Glückstraße 6, 91054 Erlangen, Germany
[5]Department for Rheumatology and Immunology, Hannover Medical School, Carl-Neuberg-Straße 1, 30625 Hannover, Germany
[6]Lead contact
*Correspondence: spoehlmann@dpz.eu (S.P.), mhoffmann@dpz.eu (M.H.)
https://doi.org/10.1016/j.celrep.2021.109825

SUMMARY

The Delta variant of severe acute respiratory syndrome coronavirus 2 (SARS-CoV-2), B.1.617.2, emerged in India and has spread to over 80 countries. B.1.617.2 replaced B.1.1.7 as the dominant virus in the United Kingdom, resulting in a steep increase in new infections, and a similar development is expected for other countries. Effective countermeasures require information on susceptibility of B.1.617.2 to control by antibodies elicited by vaccines and used for coronavirus disease 2019 (COVID-19) therapy. We show, using pseudotyping, that B.1.617.2 evades control by antibodies induced upon infection and BNT162b2 vaccination, although to a lesser extent as compared to B.1.351. We find that B.1.617.2 is resistant against bamlanivimab, a monoclonal antibody with emergency use authorization for COVID-19 therapy. Finally, we show increased Calu-3 lung cell entry and enhanced cell-to-cell fusion of B.1.617.2, which may contribute to augmented transmissibility and pathogenicity of this variant. These results identify B.1.617.2 as an immune evasion variant with increased capacity to enter and fuse lung cells.

INTRODUCTION

Vaccines based on inactivated whole virus, adenoviral vectors, or mRNAs encoding the severe acute respiratory syndrome coronavirus 2 (SARS-CoV-2) spike (S) protein protect against coronavirus disease 2019 (COVID-19) and allow effective combat against the COVID-19 pandemic (Golob et al., 2021; Polack et al., 2020; Xia et al., 2021). One key feature of these vaccines is their ability to induce the production of neutralizing antibodies in vaccinated individuals. These antibodies interfere with the ability of the S protein to drive viral entry into cells and can exhibit different modes of action. For one, antibodies targeting the receptor binding domain (RBD) can directly block S protein binding to its cellular receptor angiotensin-converting enzyme 2 (ACE2) (Barnes et al., 2020). Furthermore, antibodies directed against epitopes outside the RBD, mainly within the N-terminal domain of the S1 subunit, may sterically block S protein binding to ACE2, lock the S protein in a conformational state that does not allow the RBD to interact with ACE2, or abrogate S protein transition from the pre-fusion to the post-fusion conformation (Chi et al., 2020; Liu et al., 2020; Suryadevara et al., 2021).

Current vaccines present the S proteins of viruses circulating early during the pandemic as antigens to the immune system. However, at a later stage of the pandemic, so-called SARS-CoV-2 variants of concern (VOCs) emerged that harbor mutations in the S protein that allow for augmented transmissibility (B.1.1.7, Alpha variant) and/or immune evasion (B.1.351, Beta variant; P.1, Gamma variant) (Plante et al., 2021b). Mutations conferring increased transmissibility might augment binding to the cellular receptor ACE2, while mutations conferring immune evasion alter epitopes of neutralizing antibodies (Plante et al., 2021b). Immune evasion can allow for the infection of convalescent or vaccinated individuals, but vectored and mRNA-based vaccines protect against severe COVID-19 induced by Alpha, Beta, and Gamma VOCs.

A massive surge of COVID-19 cases was detected in India between April and May 2021 and was associated with spread of a new variant, B.1.617, that subsequently branched off into B.1.617.1 (or Kappa variant), B.1.617.2 (or Delta variant), and B.1.617.3 variants. The B.1.617.2 variant subsequently spread into more than 80 countries and became dominant in India and the United Kingdom (Campbell et al., 2021; Singh et al., 2021).
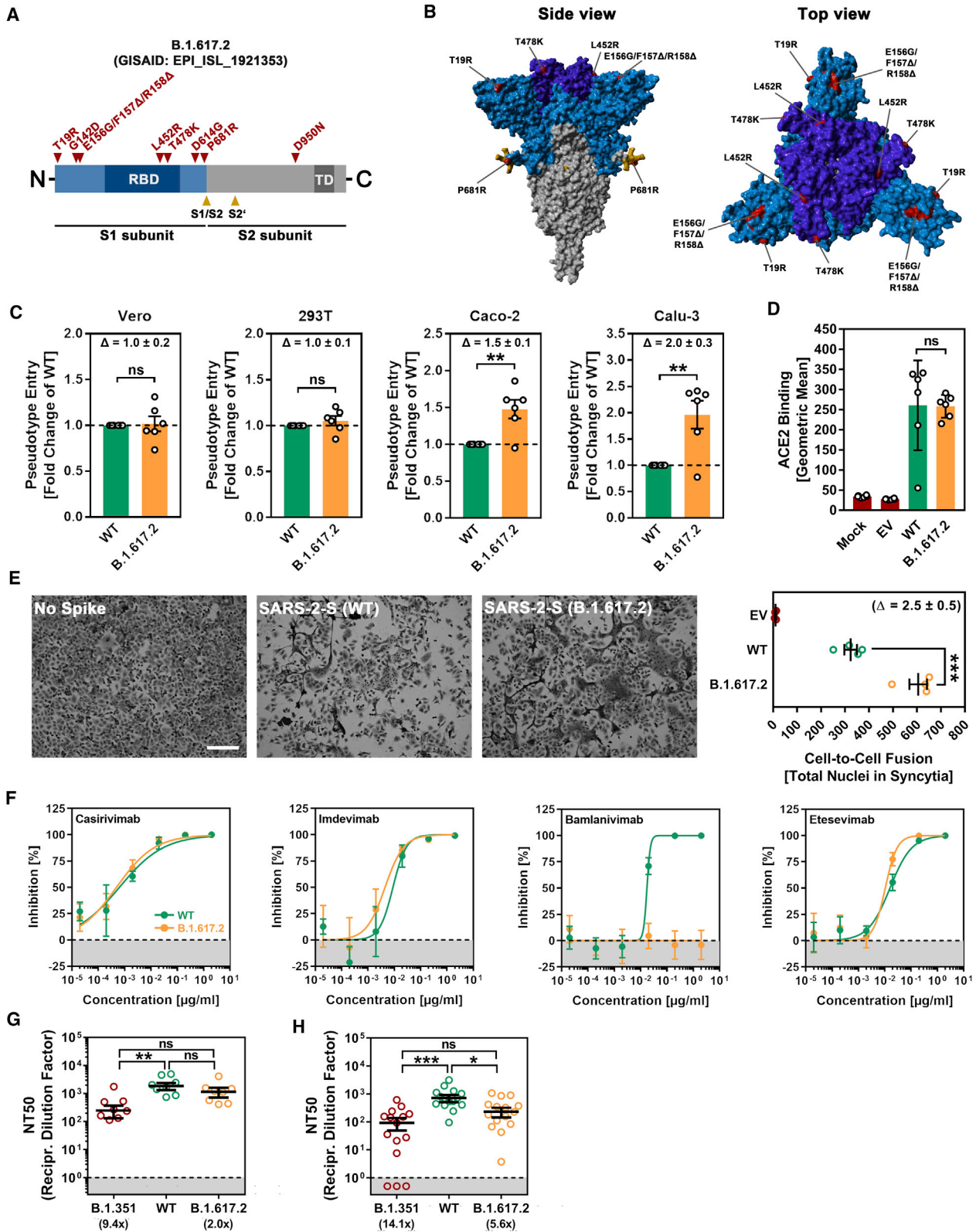
(legend on next page)

In the United Kingdom, the spread of B.1.617.2 was associated with a marked increase in cases, and more than 80% of new infections are now due to B.1.617.2. A rapid increase of B.1.617.2 spread is also expected in Germany, the United States, and several other countries, and a recent massive increase of cases in Lisbon, Portugal, that required travel restrictions is believed to be due to B.1.617.2. In order to contain the spread of B.1.617.2, now considered a VOC, it will be critical to determine whether convalescent or vaccinated patients are protected against infection by this variant. Here, we addressed this question using reporter particles pseudotyped with the SARS-CoV-2 S protein, which are suitable tools to study SARS-CoV-2 neutralization by antibodies (Riepler et al., 2020; Schmidt et al., 2020).

RESULTS

With respect to the S protein of the ancestral Wuhan-1 isolate (GISAID accession ID:EPI_ISL_406798), the S protein of B.1.617.2 harbors nine mutations in the surface unit, S1, of the S protein and 1 mutation in the transmembrane unit, S2 (Figures 1A and 1B). Mutations T19R, G142D, E156G, F157Δ, and R158Δ are located in the N-terminal domain of S1, which contains epitopes for neutralizing antibodies (Chi et al., 2020; Liu et al.,

2020; McCallum et al., 2021; Suryadevara et al., 2021). The RBD harbors mutations L452R and T478K. The mutation L452R reduces antibody-mediated neutralization (Deng et al., 2021; Liu et al., 2021b), and it has been speculated that T478K might increase infectivity (Wang et al., 2021). The mutation D614G is located between the RBD and the S1/S2 cleavage site and is linked to increased ACE2 binding, replication in the upper respiratory tract, and transmission (Figures 1A and 1B; Plante et al., 2021a; Zhou et al., 2021). Finally, P681R might increase cleavage of S protein at the S1/S2 site, while the impact of D950N on S protein-driven entry and its inhibition by antibodies is unknown.

We first asked whether the B.1.617.2 S protein mediates robust entry into cell lines frequently used for SARS-CoV-2 research, Vero (African green monkey, kidney), 293T (human, kidney), Caco-2 (human, colon), and Calu-3 (human, lung). All cell lines express endogenous ACE2 and Vero, Caco-2, and Calu-3 cells are often used for infection studies with authentic SARS-CoV-2. The B.1.617.2 S protein mediated entry into 293T and Vero cells with the same efficiency as the wild-type (WT) S protein, while entry into Caco-2 (∼1.5-fold) and Calu-3 cells (∼2.0-fold) was augmented (Figures 1C and S1A). The lung is the central target of SARS-CoV-2, but infection of the

Figure 1. The spike protein of SARS-CoV-2 B.1.617.2 promotes efficient entry into human lung and colon cells, causes more cell-to-cell fusion, and evades antibody-mediated neutralization

(A) Schematic overview of the S protein from SARS-CoV-2 variant B.1.617.2. RBD, receptor-binding domain; TD, transmembrane domain.

(B) Location of the mutations found in SARS-CoV-2 variant B.1.617.2 in the context of the trimeric spike protein (color code: light blue, S1 subunit with RBD in dark blue; gray, S2 subunit; orange, S1/S2 and S2′ cleavage sites; red, mutated amino acid residues).

(C) Pseudotyped particles bearing the S protein of wild-type (WT) SARS-CoV-2 or variant B.1.617.2 were inoculated onto the indicated cell lines, and transduction efficiency was quantified by measuring virus-encoded luciferase activity in cell lysates at 16 to 18 h post transduction. Presented are the average (mean) data from 6 biological replicates (each conducted with technical quadruplicates) for which transduction was normalized against SARS-CoV-2 S WT (= 1). Error bars indicate the standard error of the mean (SEM). Statistical significance of differences between WT and B.1.617.2 S proteins was analyzed by two-tailed Student's t test (p > 0.05, not significant [ns]; **p ≤ 0.01). See also Figure S1A.

(D) BHK-21 expressing the S protein of WT SARS-CoV-2 or variant B.1.617.2 were subsequently incubated with soluble ACE2 (harboring a C-terminal Fc-tag derived from human IgG) and AlexaFluor-488-conjugated anti-human antibody before being subjected to flow cytometry. ACE2 binding efficiency was analyzed by measuring the geometric mean channel fluorescence at 488 nm. Untransfected cells and cells transfected with empty expression plasmid served as controls. Presented are the average (mean) data from 6 biological replicates (each conducted with single samples). Error bars indicate the standard deviation (SD). Statistical significance of differences between WT and variant B.1.617.2 S proteins was analyzed by two-tailed Student's t test (p > 0.05, ns).

(E) Analysis of S protein-induced cell-to-cell fusion. A549-ACE2 cells were transfected with expression plasmid for the indicated S proteins or empty vector (EV). At 24 h post transfection, cells were fixed and subsequently stained with May-Gruenwald and Giemsa solutions.

Presented are representative microscopic images (scale bar, 200 μm). For quantification of fusion efficiency, the total number of nuclei in syncytia per image was counted. Presented are the average (mean) data from 4 biological replicates (each conducted with single samples; for each sample, 3 randomly selected areas were imaged and independently analyzed by 2 persons). Error bars indicate the SEM. Statistical significance of differences between WT and B.1.617.2 S proteins was analyzed by two-tailed Student's t test (***p ≤ 0.001).

(F) Neutralization of particles bearing SARS-CoV-2 WT or B.1.617.2 S proteins by monoclonal antibodies used for COVID-19 therapy. Pseudotyped particles bearing the S protein of WT SARS-CoV-2 or variant B.1.617.2 were incubated for 30 min at 37°C in the presence of escalating concentrations (0.00002, 0.0002, 0.002, 0.02, 0.2, and 2 μg/mL) of the indicated SARS-CoV-2 S protein-specific monoclonal antibody (please see Figure S1B) or an unrelated control antibody (please see Figure S1C) before being inoculated onto Vero cells. Transduction efficiency was quantified by measuring virus-encoded luciferase activity in cell lysates at 16 to 18 h post transduction. Presented are the average (mean) data from a single biological replicate (conducted with technical quadruplicates) for which transduction was normalized against samples that did not contain any antibody (= 0% inhibition). Error bars indicate the SD. The results were confirmed in a separate experiment.

(G) Neutralization of particles bearing SARS-CoV-2 WT, B.1.351, or B.1.617.2 S proteins by antibodies in convalescent plasma. Pseudotyped particles bearing the S protein of SARS-CoV-2 WT, B.1.351 or B.1.617.2 were incubated for 30 min at 37°C in the presence of different dilutions of convalescent plasma (1:25, 1:100, 1:400, 1:1,600, 1:6,400, and 1:25,600). Transduction efficiency was quantified by measuring virus-encoded luciferase activity in cell lysates at 16 to 18 h post transduction and used to calculate the plasma dilution factor that leads to 50% reduction in S protein-driven cell entry (neutralizing titer 50 [NT50]). Presented are the data from a single biological replicate (conducted with technical quadruplicates) for a total of 8 convalescent plasma (black lines indicate the median; error bars indicate the SEM). Statistical significance of differences between the indicated groups was analyzed by Kruskal-Wallis analysis with Dunn's post hoc test (p > 0.05, ns; *p ≤ 0.05; **p ≤ 0.01; ***p ≤ 0.001). Please see also Figure S1D.

(H) The experiment was performed as described for (G), but this time serum from Comirnaty/BNT162b2-vaccinated individuals was investigated. Presented are the data from a single biological replicate (conducted with technical quadruplicates) for a total of 15 vaccinee sera (black lines indicate the median; error bars indicate the SEM). Please see also Figure S1E.

colon has also been reported, suggesting that B.1.617.2 might have an increased capacity to enter target cells in these tissues. Finally, we did not detect increased ACE2 binding of the B.1.617.2 S protein (Figure 1D), suggesting that increased entry into Caco-2 and Calu-3 cells was not due to augmented ACE2 binding.

Besides its ability to drive fusion of viral and cellular membranes, the S protein is further able to drive the fusion of neighboring cells, resulting in the formation of multinucleated giant cells, so called syncytia, which have been observed *in vitro* following directed S protein expression or SARS-CoV-2 infection and in postmortem tissues from COVID-19 patients (Bussani et al., 2020; Tian et al., 2020; Xu et al., 2020). Since SARS-CoV-2 S protein-driven syncytium formation is believed to contribute to COVID-19 pathogenesis, we investigated the ability of the B.1.617.2 S protein to drive cell-to-cell fusion in the human lung cell line A549, which was engineered to express high levels of ACE2. As expected, directed expression of WT S led to the formation of syncytia, while syncytia formation was not observed when cells were transfected with empty expression plasmid (Figure 1E). Strikingly, directed expression of the B.1.617.2 S protein caused more and larger syncytia, and quantification of cell-to-cell fusion revealed that fusion by the B.1.617.2 S protein was ~2.5-fold more effective as compared to the WT S protein (Figure 1E).

We next determined whether entry of B.1.617.2 was susceptible to inhibition by recombinant antibodies with emergency use authorization for COVID-19 treatment (Figure S1B). Three out of four antibodies tested inhibited the B.1.617.2 S protein with similar efficiency as the WT S protein (Figures 1F and S1C). However, B.1.617.2 was resistant to bamlanivimab, most likely because of the mutation L452R (Figure S1B; Starr et al., 2021). Thus, bamlanivimab monotherapy is not suitable for prevention or treatment of B.1.617.2 infection. Finally, we asked whether B.1.617.2 entry is inhibited by antibodies generated by infected or vaccinated individuals. For these experiments, we employed the S protein of B.1.351 as control since this VOC exhibits marked evasion from neutralizing antibodies. A previously described collection of plasma (Hoffmann et al., 2021a) from convalescent COVID-19 patients collected at University Hospital Göttingen, Germany, neutralized entry driven by the B.1.617.2 S protein with a slightly reduced efficiency as compared to the WT S protein (Figures 1G and S1D). In contrast, neutralization of the B.1.351 S protein-dependent entry was markedly reduced. Finally, similar observations were made with previously characterized sera (Hoffmann et al., 2021b) from donors who received two doses of BNT162b2, although immune evasion of B.1.617.2 was more prominent as compared to convalescent sera (Figures 1H and S1E).

DISCUSSION

Our results demonstrate immune evasion, enhanced colon- and lung cell entry, and augmented syncytium formation by B.1.617.2. Evasion of antibody-mediated neutralization by B.1.617.2 is in agreement with two recent studies (Liu et al., 2021a; Wall et al., 2021), and although it is more prominent than previously observed by us for B.1.1.7, it is clearly less prom-

inent as compared to B.1.351 (Hoffmann et al., 2021a). This finding would be compatible with increased vaccine breakthrough of B.1.617.2 but also suggests that BNT162b2 should still protect from B.1.617.2-induced COVID-19. Treatment of infection with bamlanivimab alone will be ineffective, but our data indicate that casirivimab, imdevimab, and etesevimab will remain effective treatment options for B.1.617.2-infected patients, especially when administered early after infection. The observation that the B.1.617.2 S protein is able to cause more cell-to-cell fusion than the WT S protein may suggest that B.1.617.2 could cause more tissue damage, and thus be more pathogenic, than previous variants, and that viral spread via syncytium formation could contribute to efficient inter- and intra-host spread of this variant. Entry experiments with cell lines need to be interpreted with care, and confirmation with primary cells is pending. However, the significantly increased entry into the colon and lung cell lines Caco-2 and Calu-3, respectively, suggests that B.1.617.2 might have an augmented capacity to infect these organs, and increased infection of the respiratory epithelium might account for the purported increased transmissibility of B.1.617.2.

STAR★METHODS

Detailed methods are provided in the online version of this paper and include the following:

- KEY RESOURCES TABLE
- RESOURCE AVAILABILITY
  - Lead contact
  - Materials availability
  - Data and code availability
- EXPERIMENTAL MODEL AND SUBJECT DETAILS
  - Cell culture
- METHOD DETAILS
  - Expression plasmids
  - Sequence analysis and protein models
  - Production of pseudotype particles
  - Transduction of target cells
  - Analysis of ACE2 binding
  - Syncytium formation assay
  - Collection of serum and plasma samples
  - Neutralization assay
- QUANTIFICATION AND STATISTICAL ANALYSIS

REFERENCES

Barnes, C.O., West, A.P., Jr., Huey-Tubman, K.E., Hoffmann, M.A.G., Sharaf, N.G., Hoffman, P.R., Koranda, N., Gristick, H.B., Gaebler, C., Muecksch, F., et al. (2020). Structures of Human Antibodies Bound to SARS-CoV-2 Spike Reveal Common Epitopes and Recurrent Features of Antibodies. Cell *182*, 828–842.e16.

Berger Rentsch, M., and Zimmer, G. (2011). A vesicular stomatitis virus repli-con-based bioassay for the rapid and sensitive determination of multi-species type I interferon. PLoS ONE *6*, e25858.

Bussani, R., Schneider, E., Zentilin, L., Collesi, C., Ali, H., Braga, L., Volpe, M.C., Colliva, A., Zanconati, F., Berlot, G., et al. (2020). Persistence of viral RNA, pneumocyte syncytia and thrombosis are hallmarks of advanced COVID-19 pathology. EBioMedicine *61*, 103104.

Cai, Y., Zhang, J., Xiao, T., Peng, H., Sterling, S.M., Walsh, R.M., Jr., Rawson, S., Rits-Volloch, S., and Chen, B. (2020). Distinct conformational states of SARS-CoV-2 spike protein. Science *369*, 1586–1592.

Campbell, F., Archer, B., Laurenson-Schafer, H., Jinnai, Y., Konings, F., Batra, N., Pavlin, B., Vandemaele, K., Van Kerkhove, M.D., Jombart, T., et al. (2021). Increased transmissibility and global spread of SARS-CoV-2 variants of concern as at June 2021. Euro Surveill. *26*, 2100509.

Chi, X., Yan, R., Zhang, J., Zhang, G., Zhang, Y., Hao, M., Zhang, Z., Fan, P., Dong, Y., Yang, Y., et al. (2020). A neutralizing human antibody binds to the N-terminal domain of the Spike protein of SARS-CoV-2. Science *369*, 650–655.

Deng, X., Garcia-Knight, M.A., Khalid, M.M., Servellita, V., Wang, C., Morris, M.K., Sotomayor-González, A., Glasner, D.R., Reyes, K.R., Gliwa, A.S., et al. (2021). Transmission, infectivity, and neutralization of a spike L452R SARS-CoV-2 variant. Cell *184*, 3426–3437.e8.

Golob, J.L., Lugogo, N., Lauring, A.S., and Lok, A.S. (2021). SARS-CoV-2 vaccines: a triumph of science and collaboration. JCI Insight *6*, e149187.

Hansen, J., Baum, A., Pascal, K.E., Russo, V., Giordano, S., Wloga, E., Fulton, B.O., Yan, Y., Koon, K., Patel, K., et al. (2020). Studies in humanized mice and convalescent humans yield a SARS-CoV-2 antibody cocktail. Science *369*, 1010–1014.

Hoffmann, M., Kleine-Weber, H., Schroeder, S., Krüger, N., Herrler, T., Erichsen, S., Schiergens, T.S., Herrler, G., Wu, N.H., Nitsche, A., et al. (2020). SARS-CoV-2 Cell Entry Depends on ACE2 and TMPRSS2 and Is Blocked by a Clinically Proven Protease Inhibitor. Cell *181*, 271–280.e8.

Hoffmann, M., Arora, P., Groß, R., Seidel, A., Hörnich, B.F., Hahn, A.S., Krüger, N., Graichen, L., Hofmann-Winkler, H., Kempf, A., et al. (2021a). SARS-CoV-2

variants B.1.351 and P.1 escape from neutralizing antibodies. Cell *184*, 2384–2393.e12.

Hoffmann, M., Hofmann-Winkler, H., Krüger, N., Kempf, A., Nehlmeier, I., Graichen, L., Sidarovich, A., Moldenhauer, A.-S., Winkler, M.S., Schulz, S., et al. (2021b). SARS-CoV-2 variant B.1.617 is resistant to Bamlanivimab and evades antibodies induced by infection and vaccination. bioRxiv. https://doi.org/10.1101/2021.2005.2004.442663.

Jones, B.E., Brown-Augsburger, P.L., Corbett, K.S., Westendorf, K., Davies, J., Cujec, T.P., Wiethoff, C.M., Blackbourne, J.L., Heinz, B.A., Foster, D., et al. (2020). LY-CoV555, a rapidly isolated potent neutralizing antibody, provides protection in a non-human primate model of SARS-CoV-2 infection. bioRxiv.

Liu, L., Wang, P., Nair, M.S., Yu, J., Rapp, M., Wang, Q., Luo, Y., Chan, J.F., Sahi, V., Figueroa, A., et al. (2020). Potent neutralizing antibodies against multiple epitopes on SARS-CoV-2 spike. Nature *584*, 450–456.

Liu, J., Liu, Y., Xia, H., Zou, J., Weaver, S.C., Swanson, K.A., Cai, H., Cutler, M., Cooper, D., Muik, A., et al. (2021a). BNT162b2-elicited neutralization of B.1.617 and other SARS-CoV-2 variants. Nature *596*, 273–275.

Liu, Z., VanBlargan, L.A., Bloyet, L.M., Rothlauf, P.W., Chen, R.E., Stumpf, S., Zhao, H., Errico, J.M., Theel, E.S., Liebeskind, M.J., et al. (2021b). Identification of SARS-CoV-2 spike mutations that attenuate monoclonal and serum antibody neutralization. Cell Host Microbe *29*, 477–488.e4.

McCallum, M., De Marco, A., Lempp, F.A., Tortorici, M.A., Pinto, D., Walls, A.C., Beltramello, M., Chen, A., Liu, Z., Zatta, F., et al. (2021). N-terminal domain antigenic mapping reveals a site of vulnerability for SARS-CoV-2. Cell *184*, 2332–2347.e16.

Plante, J.A., Liu, Y., Liu, J., Xia, H., Johnson, B.A., Lokugamage, K.G., Zhang, X., Muruato, A.E., Zou, J., Fontes-Garfias, C.R., et al. (2021a). Spike mutation D614G alters SARS-CoV-2 fitness. Nature *592*, 116–121.

Plante, J.A., Mitchell, B.M., Plante, K.S., Debbink, K., Weaver, S.C., and Menachery, V.D. (2021b). The variant gambit: COVID-19's next move. Cell Host Microbe *29*, 508–515.

Polack, F.P., Thomas, S.J., Kitchin, N., Absalon, J., Gurtman, A., Lockhart, S., Perez, J.L., Pérez Marc, G., Moreira, E.D., Zerbini, C., et al.; C4591001 Clinical Trial Group (2020). Safety and Efficacy of the BNT162b2 mRNA Covid-19 Vaccine. N. Engl. J. Med. *383*, 2603–2615.

Riepler, L., Rössler, A., Falch, A., Volland, A., Borena, W., von Laer, D., and Kimpel, J. (2020). Comparison of Four SARS-CoV-2 Neutralization Assays. Vaccines (Basel) *9*, 13.

Schmidt, F., Weisblum, Y., Muecksch, F., Hoffmann, H.H., Michailidis, E., Lorenzi, J.C.C., Mendoza, P., Rutkowska, M., Bednarski, E., Gaebler, C., et al. (2020). Measuring SARS-CoV-2 neutralizing antibody activity using pseudotyped and chimeric viruses. J. Exp. Med. *217*, e20201181.

Shi, R., Shan, C., Duan, X., Chen, Z., Liu, P., Song, J., Song, T., Bi, X., Han, C., Wu, L., et al. (2020). A human neutralizing antibody targets the receptor-binding site of SARS-CoV-2. Nature *584*, 120–124.

Singh, J., Rahman, S.A., Ehtesham, N.Z., Hira, S., and Hasnain, S.E. (2021). SARS-CoV-2 variants of concern are emerging in India. Nat. Med. *27*, 1131–1133.

Starr, T.N., Greaney, A.J., Dingens, A.S., and Bloom, J.D. (2021). Complete map of SARS-CoV-2 RBD mutations that escape the monoclonal antibody LY-CoV555 and its cocktail with LY-CoV016. Cell Rep Med *2*, 100255.

Suryadevara, N., Shrihari, S., Gilchuk, P., VanBlargan, L.A., Binshtein, E., Zost, S.J., Nargi, R.S., Sutton, R.E., Winkler, E.S., Chen, E.C., et al. (2021). Neutralizing and protective human monoclonal antibodies recognizing the N-terminal domain of the SARS-CoV-2 spike protein. Cell *184*, 2316–2331.e15.

Tian, S., Hu, W., Niu, L., Liu, H., Xu, H., and Xiao, S.Y. (2020). Pulmonary Pathology of Early-Phase 2019 Novel Coronavirus (COVID-19) Pneumonia in Two Patients With Lung Cancer. J. Thorac. Oncol. *15*, 700–704.

Wall, E.C., Wu, M., Harvey, R., Kelly, G., Warchal, S., Sawyer, C., Daniels, R., Hobson, P., Hatipoglu, E., Ngai, Y., et al. (2021). Neutralising antibody activity against SARS-CoV-2 VOCs B.1.617.2 and B.1.351 by BNT162b2 vaccination. Lancet *397*, 2331–2333.

Wang, R., Chen, J., Gao, K., and Wei, G.W. (2021). Vaccine-escape and fast-growing mutations in the United Kingdom, the United States, Singapore, Spain, India, and other COVID-19-devastated countries. Genomics *113*, 2158–2170.

Xia, S., Zhang, Y., Wang, Y., Wang, H., Yang, Y., Gao, G.F., Tan, W., Wu, G., Xu, M., Lou, Z., et al. (2021). Safety and immunogenicity of an inactivated SARS-CoV-2 vaccine, BBIBP-CorV: a randomised, double-blind, placebo-controlled, phase 1/2 trial. Lancet Infect. Dis. *21*, 39–51.

Xu, Z., Shi, L., Wang, Y., Zhang, J., Huang, L., Zhang, C., Liu, S., Zhao, P., Liu, H., Zhu, L., et al. (2020). Pathological findings of COVID-19 associated with acute respiratory distress syndrome. Lancet Respir. Med. *8*, 420–422.

Zhou, B., Thao, T.T.N., Hoffmann, D., Taddeo, A., Ebert, N., Labroussaa, F., Pohlmann, A., King, J., Steiner, S., Kelly, J.N., et al. (2021). SARS-CoV-2 spike D614G change enhances replication and transmission. Nature *592*, 122–127.

STAR★METHODS

KEY RESOURCES TABLE

REAGENT or RESOURCE	SOURCE	IDENTIFIER
Antibodies		
Casirivimab	Laboratory of Hans-Martin Jäck	N/A
Imdevimab	Laboratory of Hans-Martin Jäck	N/A
Bamlanivimab	Laboratory of Hans-Martin Jäck	N/A
Etesevimab	Laboratory of Hans-Martin Jäck	N/A
hIgG	Laboratory of Hans-Martin Jäck	N/A
Goat anti-Human IgG (H+L) Cross-Adsorbed Secondary Antibody, Alexa Fluor 488	Thermo Fisher Scientific	Cat# A-11013; RRID: AB_2534080
Anti-VSV-G antibody (I1, produced from CRL-2700 mouse hybridoma cells)	ATCC	Cat# CRL-2700; RRID: CVCL_G654
Bacterial and virus strains		
VSV*ΔG-FLuc	Laboratory of Gert Zimmer	N/A
One Shot OmniMAX 2 T1R Chemically Competent *E. coli*	Thermo Fisher Scientific	Cat# C854003
Biological samples		
Patient Plasma (SI 15)	Laboratory of Martin Sebastian Winkler	N/A
Patient Plasma (SI 18)	Laboratory of Martin Sebastian Winkler	N/A
Patient Plasma (SI 22)	Laboratory of Martin Sebastian Winkler	N/A
Patient Plasma (SI 23)	Laboratory of Martin Sebastian Winkler	N/A
Patient Plasma (SI 24)	Laboratory of Martin Sebastian Winkler	N/A
Patient Plasma (SI 27)	Laboratory of Martin Sebastian Winkler	N/A
Patient Plasma (SI 33)	Laboratory of Martin Sebastian Winkler	N/A
Patient Plasma (SI 51)	Laboratory of Martin Sebastian Winkler	N/A
Vaccinee Serum (ID4844)	Laboratory of Georg M.N. Behrens	N/A
Vaccinee Serum (ID4846)	Laboratory of Georg M.N. Behrens	N/A
Vaccinee Serum (ID4847)	Laboratory of Georg M.N. Behrens	N/A
Vaccinee Serum (ID4848)	Laboratory of Georg M.N. Behrens	N/A
Vaccinee Serum (ID4849)	Laboratory of Georg M.N. Behrens	N/A
Vaccinee Serum (ID4863)	Laboratory of Georg M.N. Behrens	N/A
Vaccinee Serum (ID4864)	Laboratory of Georg M.N. Behrens	N/A
Vaccinee Serum (ID4865)	Laboratory of Georg M.N. Behrens	N/A
Vaccinee Serum (ID4866)	Laboratory of Georg M.N. Behrens	N/A
Vaccinee Serum (ID4867)	Laboratory of Georg M.N. Behrens	N/A
Vaccinee Serum (ID4868)	Laboratory of Georg M.N. Behrens	N/A
Vaccinee Serum (ID4872)	Laboratory of Georg M.N. Behrens	N/A
Vaccinee Serum (ID4874)	Laboratory of Georg M.N. Behrens	N/A
Vaccinee Serum (ID4876)	Laboratory of Georg M.N. Behrens	N/A
Vaccinee Serum (ID4877)	Laboratory of Georg M.N. Behrens	N/A
Chemicals, peptides, and recombinant proteins		
Soluble human ACE2 (sol-hACE2-Fc)	Laboratory of Stefan Pöhlmann	N/A
Critical commercial assays		
Beetle-Juice Kit	PJK	Cat# 102511
Experimental models: Cell lines		
293T	DSMZ	Cat# ACC-635; RRID: CVCL_0063
A549 (ACE2)	Laboratory of Stefan Pöhlmann	N/A

Continued

REAGENT or RESOURCE	SOURCE	IDENTIFIER
BHK-21	Laboratory of Georg Herrler	ATCC Cat# CCL-10; RRID:CVCL_1915
Caco-2	Laboratory of Stefan Pöhlmann	ATCC Cat# HTB-37; RRID: CVCL_0025
Calu-3	Laboratory of Stephan Ludwig	ATCC Cat# HTB-55; RRID: CVCL_0609
Vero76	Laboratory of Andrea Maisner	ATCC Cat# CRL-1586; RRID: CVCL_0574
Oligonucleotides		
SARS-2-S (BamHI) F (AAGGCCGGATCCGCCACCATGTTCGTGTTTCTGGTGCTGC)	Sigma-Aldrich	N/A
SARS-2-SΔ18 (XbaI) R (AAGGCCTCTAGACTACTTGCAGCAGCTGCCACAG)	Sigma-Aldrich	N/A
SARS-2-S (T19R) F (GTGAACCTGCGCACAAGAACCCAGCTGCCTCCAGC)	Sigma-Aldrich	N/A
SARS-2-S (T19R) R (GTTCTTGTGCGCAGGTTCACACACTGGCTGGAC)	Sigma-Aldrich	N/A
SARS-2-S (E142D) F (CCTTCCTGGACGTCTACTATCACAAGAAC)	Sigma-Aldrich	N/A
SARS-2-S (E142D) R (TAGTAGACGTCCAGGAAGGGGTCGTTGCAGAAC)	Sigma-Aldrich	N/A
SARS-2-S (E142D/E156G/F157Δ/R158Δ) Hyb F (GTTCTGCAACGACCCCTTCCTGGACGTCTACTATCACAAGAACAACAAGAGCTGG)	Sigma-Aldrich	N/A
SARS-2-S (E142D/E156G/F157Δ/R158Δ) Hyb R (CAGTTGTTGGCGCTGCTGTACACCCCGCTTTCCATCCAGCTCTTGTTGTTCTTGTGATAG)	Sigma-Aldrich	N/A
SARS-2-S (E156G/F157Δ/R158Δ) F (TGGAAAGCGGGGTGTACAGCAGCGCCAACAACTGC)	Sigma-Aldrich	N/A
SARS-2-S (E156G/F157Δ/R158Δ) R (GCTGTACACCCCGCTTTCCATCCAGCTCTTGTTG)	Sigma-Aldrich	N/A
SARS-2-S (L452R) F (TACAATTACCGGTACCGGCTGTTCCGGAAGTC)	Sigma-Aldrich	N/A
SARS-2-S (L452R) R (CAGCCGGTACcGGTAATTGTAGTTGCCGCCGAC)	Sigma-Aldrich	N/A
SARS-2-S (L452R/T478K) Hyb F (ACAATTACCGGTACCGGCTGTTCCGGAAGTCCAATCTGAAGCCCTTCGAGCGGGACATC)	Sigma-Aldrich	N/A
SARS-2-S (L452R/T478K) Hyb R (TTACAAGGTTTGCTGCCGGCCTGATAGATCTCGGTGGAGATGTCCCGCTCGAAGGGCTTC)	Sigma-Aldrich	N/A
SARS-2-S (T478K) F (CCGGCAGCAAACCTTGTAACGGCGTGGAAGGCTTC)	Sigma-Aldrich	N/A
SARS-2-S (T478K) R (GTTACAAGGTTTGCTGCCGGCCTGATAGATCTCG)	Sigma-Aldrich	N/A
SARS-2-S (P681R) F (CAAACAGCCGCAGACGGGCCAGATCTGTG)	Sigma-Aldrich	N/A
SARS-2-S (P681R) R (GCCCGTCTGCGGCTGTTTGTCTGTGTCTG)	Sigma-Aldrich	N/A

(Continued on next page)

Continued

REAGENT or RESOURCE	SOURCE	IDENTIFIER
SARS-2-S (D950N) F (AAGCTGCAGAA CGTGGTCAACCAGAATGCCCAGG)	Sigma-Aldrich	N/A
SARS-2-S (D950N) R (TGACCACGTTCT GCAGCTTTCCCAGGGCGCTTGC)	Sigma-Aldrich	N/A
SARS-2-S Seq-01 (CAAGATCTACAGCAAGCACACC)	Sigma-Aldrich	N/A
SARS-2-S Seq-02 (GTCGGCGGCAACTACAATTAC)	Sigma-Aldrich	N/A
SARS-2-S Seq-03 (CTGTCTGATCGGAGCCGAGCAC)	Sigma-Aldrich	N/A
SARS-2-S Seq-04 (TGAGATGATCGCCCAGTACAC)	Sigma-Aldrich	N/A
SARS-2-S Seq-05 (GCCATCTGCCACGACGGCAAAG)	Sigma-Aldrich	N/A
pCG1 F (CCTGGGCAACGTGCTGGT)	Sigma-Aldrich	N/A
pCG1 R (GTCAGATGCTCAAGGGGCTTCA)	Sigma-Aldrich	N/A
Recombinant DNA		
Plasmid: pCG1	Laboratory of Roberto Cattaneo	N/A
Plasmid: pCAGGS-VSV-G	Laboratory of Stefan Pöhlmann	N/A
Plasmid: pCAGGS-DsRed	Laboratory of Stefan Pöhlmann	N/A
Plasmid: pCG1-SARS-2-SΔ18 (D614G), codon-optimized	Laboratory of Stefan Pöhlmann	N/A
Plasmid: pCG1-SARS-2-SΔ18 (B.1.351), codon-optimized	Laboratory of Stefan Pöhlmann	N/A
Plasmid: pCG1-SARS-2-SΔ18 (B.1.617.2), codon-optimized	Laboratory of Stefan Pöhlmann	N/A
Plasmid: pCG1-solACE2-Fc	Laboratory of Stefan Pöhlmann	N/A
Software and algorithms		
Hidex Sense Microplate Reader Software	Hidex Deutschland Vertrieb GmbH	https://www.hidex.de
YASARA (version 19.1.27)	YASARA Biosciences GmbH	http://www.yasara.org
Adobe Photoshop CS5 Extended (version 12.0 × 32)	Adobe	https://www.adobe.com/
GraphPad Prism (version 8.3.0(538))	GraphPad Software	https://www.graphpad.com/
ZEN imaging software	Carl Zeiss	https://www.zeiss.com/corporate/int/home.html
Microsoft Office Standard 2010 (version 14.0.7232.5000)	Microsoft Corporation	https://www.microsoft.com/microsoft-365
Other		
Complex of SARS-CoV-2 receptor binding domain with the Fab fragments of two neutralizing antibodies (PDB: 6XDG)	Hansen et al., 2020	https://www.rcsb.org/structure/6XDG
SARS-CoV 2 Spike Protein bound to LY-CoV555 (PDB: 7L3N)	Jones et al., 2020	https://www.rcsb.org/structure/7L3N
Molecular basis for a potent human neutralizing antibody targeting SARS-CoV-2 RBD (PDB: 7C01)	Shi et al., 2020	https://www.rcsb.org/structure/7C01
Distinct conformational states of SARS-CoV-2 spike protein (PDB: 6XR8)	Cai et al., 2020	https://www.rcsb.org/structure/6XR8

RESOURCE AVAILABILITY

Lead contact
Requests for material can be directed to Markus Hoffmann (mhoffmann@dpz.eu) and the lead contact, Stefan Pöhlmann (spoehlmann@dpz.eu).

Materials availability
All materials and reagents will be made available upon installment of a material transfer agreement (MTA).

Data and code availability

- All data reported in this paper will be shared by the lead contact upon request.
- This paper does not report original code.
- Any additional information required to reanalyze the data reported in this paper is available from the lead contact upon request.

EXPERIMENTAL MODEL AND SUBJECT DETAILS

Cell culture
All cell lines were incubated at 37°C in a humidified atmosphere containing 5% CO$_2$. 293T (human, female, kidney; ACC-635, DSMZ; RRID: CVCL_0063), Vero76 cells (African green monkey kidney, female, kidney; CRL-1586, ATCC; RRID: CVCL_0574, kindly provided by Andrea Maisner), BHK-21 (Syrian hamster, male, kidney; CCL-10, ATCC; RRID: CVCL_1915, kindly provided by Georg Herrler) and A549-ACE2 cells (Hoffmann et al., 2021a), which were derived from parental A549 cells (human, male, lung; CRM-CCL-185, ATCC; RRID:CVCL_0023; kindly provided by Georg Herrler), were cultured in Dulbecco's modified Eagle medium (PAN-Biotech) supplemented with 10% fetal bovine serum (FBS, Biochrom), 100 U/ml penicillin and 0.1 mg/ml streptomycin (pen/strep) (PAN-Biotech). In addition, Calu-3 (human, male, lung; HTB-55, ATCC; RRID: CVCL_0609, kindly provided by Stephan Ludwig) and Caco-2 cells (human, male, colon; HTB-37, ATCC, RRID: CVCL_0025) were cultured in minimum essential medium (GIBCO) supplemented with 10% FBS, 1% pen/strep, 1x non-essential amino acid solution (from 100x stock, PAA) and 1 mM sodium pyruvate (Thermo Fisher Scientific). Cell lines were validated by STR-typing, amplification and sequencing of a fragment of the cytochrome *c* oxidase gene, microscopic examination and/or according to their growth characteristics. Furthermore, all cell lines were routinely tested for contamination by mycoplasma contamination.

METHOD DETAILS

Expression plasmids
Plasmids encoding pCAGGS-DsRed, pCAGGS-VSV-G (vesicular stomatitis virus glycoprotein), pCG1-WT SARS-CoV-2 S (codon optimized, based on the Wuhan/Hu-1/2019 isolate, equipped with D614G mutation; with C-terminal truncation of the last 18 amino acid), pCG1-SARS-CoV-2 S B.1.351 (codon optimized; with C-terminal truncation of the last 18 amino acid), ACE2 (angiotensin converting enzyme 2) and soluble ACE2 have been previously described (Hoffmann et al., 2020, 2021a, 2021b). In order to generate the expression vector for the S protein of SARS-CoV-2 variant B.1.617.2, the respective mutations were inserted into the WT SARS-CoV-2 S sequence by splice-overlap PCR. The resulting open reading frame was further inserted into vector pCG1 plasmid (kindly provided by Roberto Cattaneo, Mayo Clinic College of Medicine, Rochester, MN, USA), using BamHI and XbaI restriction enzymes. The integrity of all sequences was confirmed by sequence analysis using a commercial sequencing service (Microsynth SeqLab). Specific details on the cloning procedure can be obtained upon request. Transfection of 293T cells was carried out by the calcium-phosphate precipitation method, while BHK-21 and A549-ACE2 cells were transfected using Lipofectamine LTX (Thermo Fisher Scientific).

Sequence analysis and protein models
The S protein sequence of SARS-CoV-2 S variant B.1.617.2 (GISAID Accession ID: EPI_ISL_1921353) was obtained from the GISAID (global initiative on sharing all influenza data) databank (https://www.gisaid.org/). Protein models were generated employing the YA-SARA software (http://www.yasara.org/index.html) and are based on published crystal structure PDB: 6XDG (Hansen et al., 2020), PDB: 7L3N (Jones et al., 2020) or PDB: 7C01 (Shi et al., 2020), or a template that was constructed by modeling the SARS-2 S sequence on PDB: 6XR8 (Cai et al., 2020), using the SWISS-MODEL online tool (https://swissmodel.expasy.org)

Production of pseudotype particles
Rhabdoviral pseudotypes bearing SARS-CoV-2 spike protein were generated according to an established protocol (Berger Rentsch and Zimmer, 2011). Briefly, 293T cells were transfected with expression plasmids encoding S protein, VSV-G or empty plasmid (control). At 24 h posttransfection, cells were inoculated with a replication-deficient vesicular stomatitis virus that lacks the genetic information for VSV-G and instead codes for two reporter proteins, enhanced green fluorescent protein and firefly luciferase (FLuc),

VSV*ΔG-FLuc (kindly provided by Gert Zimmer) at a multiplicity of infection of 3. Following 1 h of incubation at 37°C, the inoculum was removed and cells were washed with phosphate-buffered saline (PBS). Subsequently, cells received culture medium containing anti-VSV-G antibody (culture supernatant from I1-hybridoma cells; ATCC no. CRL-2700; except for cells expressing VSV-G, which received only medium) in order to neutralize residual input virus. After 16-18 h, the culture supernatant was harvested, clarified from cellular debris by centrifugation at 4,000 x g, 10 min, aliquoted and stored at −80°C.

Transduction of target cells

For transduction experiments, target cells were seeded in 96-well plates and inoculated with equal volumes of pseudotype particles. The transduction efficiency was evaluated at 16-18 h post transduction. For this, cells were lysed in PBS containing 0.5% Triton X-100 (Carl Roth) for 30 min at RT. Afterward, cell lysates were transferred into white 96-well plates and mixed with luciferase substrate (Beetle- Juice, PJK) before luminescence was recorded using a Hidex Sense Plate luminometer (Hidex).

Analysis of ACE2 binding

For the production of soluble ACE2 fused to the Fc portion of human immunoglobulin G (IgG), sol-ACE2, 293T cells were seeded in a T-75 flask and transfected with 20 μg of sol-ACE2 expression plasmid. The medium was replaced at 10 h posttransfection and cells were further incubated for 38 h. Further, the culture supernatant was harvested and clarified by centrifugation at 2,000 x g, 10 min, 4°C. Next, the clarified supernatant was loaded onto Vivaspin protein concentrator columns (molecular weight cut-off of 30 kDa; Sartorius) and centrifuged at 4,000 x g at 4°C until the supernatant was 100-fold concentrated. Finally, concentrated sol-ACE2 was aliquoted and stored at −80°C.

In order to test the binding efficiency of sol-ACE2 to S protein, BHK-21 cells were seeded in 12-well plates and transfected with expression plasmid for WT or SARS-CoV-2 S variant. Untransfected cells and cells transfected with empty pCG1 plasmid served as controls. At 24 h posttransfection, the culture supernatant was removed and cells were washed and resuspended in PBS and transferred into 1.5 ml reaction tubes before being pelleted by centrifugation (600 x g, 5 min, RT, all centrifugation steps). Thereafter, cells were washed with PBS containing 1% bovine serum albumin (BSA; PBS/BSA) and pelleted again by centrifugation. Next, the supernatant was removed and cell pellets were incubated with 100 μl of solACE2-Fc (1:100 in PBS/BSA) and rotated for 1 h at 4°C using a Rotospin eppi rotator disk (IKA). After incubation, cells were pelleted and incubated with 100 μl of human AlexaFluor-488-conjugated antibody (1:200 in PBS/BSA; Thermo Fisher Scientific) and rotated again as described above. Finally, cells were washed and resuspended in PBS/BSA and subjected to flow cytometry using an LSR II flow cytometer and the FACS Diva software (BD Biosciences). Data analysis was performed using the FCS express 4 Flow research software (*De Novo* Software) in order to obtain the geometric mean values.

Syncytium formation assay

In order to analyze S protein-driven cell-to-cell fusion, A549-ACE2 cells were grown in 12-well plates and transfected with expression vector for WT or B.1.617.2 S protein. In addition, cells transfected with empty plasmid served as control. At 24 h posttransfection, cells were washed with PBS and fixed by incubation (20 min, room temperature) with 4% paraformaldehyde solution (Carl Roth). Thereafter, cells were washed with deionized water, air-dried and stained with May-Gruenwald solution (30 min, room temperature; Sigma-Aldrich). Next, cells were washed three times with deionized water, air-dried and stained with 1:10 diluted Giemsa solution (30 min, room temperature; Sigma-Aldrich). Finally, cells were washed three times with deionized water, air-dried and analyzed by bright-field microscopy using a Zeiss LSM800 confocal laser scanning microscope and the ZEN imaging software (Zeiss). For each sample, three randomly selected areas were imaged and S protein-driven syncytium formation was quantified by counting the total number of nuclei in syncytia per image. Syncytia were defined as cells containing at least three nuclei. To eliminate potential bias and correct for counting errors, counting was performed blinded by two persons independently and for each sample average counts were used. Further, for each biological replicate, the average (mean) total number of nuclei in syncytia per image was calculated from three images obtained from randomly selected areas of the well.

Collection of serum and plasma samples

Before analysis, all serum and plasma samples were heat-inactivated at 56°C for 30 min. Further, all plasma/serum samples were pre-screened for their ability to neutralize transduction of Vero cells by pseudotype particles bearing WT SARS-CoV-2 S.

Convalescent plasma was obtained from COVID-19 patients treated at the intensive care unit of the University Medicine Göttingen (UMG) under approval given by the ethic committee of the UMG (SeptImmun Study 25/4/19 Ü). Cell Preparation Tube (CPT) vacutainers with sodium citrate were used for collection of convalescent plasma. Further, plasma was collected as supernatant over the peripheral blood mononuclear cell layer. In addition to convalescent plasma, serum from individuals vaccinated with BioNTech/Pfizer vaccine BNT162b2/Comirnaty was collected 24-31 days after receiving the second dose using S-Monovette® EDTA tubes (Sarstedt). Sampling and sample analysis were approved by the Institutional Review Board of Hannover Medical School (8973_BO_K_2020, amendment Dec 2020).

Neutralization assay

For neutralization experiments, S protein bearing pseudotype particles were pre-incubated for 30 min at 37°C with different concentrations of casirivimab, imdevimab, bamlanivimab, etesevimab, or unrelated control IgG (2, 0.2, 0.02, 0.002, 0.0002, 0.00002 μg/ml).

Alternatively, pseudotype particles were pre-incubated with different dilutions (1:25, 1:100, 1:400, 1:1,600 and 1:6,400) of convalescent plasma or serum from BNT162b2/Comirnaty vaccinated individuals. Following incubation, mixtures were inoculated onto Vero cells with particles incubated only with medium serving as control. Transduction efficiency was determined at 16-18 h postinoculation as described above.

QUANTIFICATION AND STATISTICAL ANALYSIS

The results on S protein-driven cell entry represent average (mean) data acquired from six biological replicates, each conducted with four technical replicates. Data were normalized against WT S protein, for which entry was set as 1. Alternatively, transduction was normalized against the background signal (luminescence measured for cells inoculated with particles bearing no viral glycoprotein; set as 1). Sol-ACE2 binding results are average (mean) data obtained from six biological replicates, each conducted with single samples. Each data point represents the geometric mean channel fluorescence for one biological replicate without normalization. Data on S protein-driven cell-to-cell fusion represent average (mean) data from four biological replicates, each conducted with single samples (three images per sample). Each data point represents the average (mean) number of nuclei in syncytia per image from two counting events by independent persons for each of the four biological replicates without normalization. The neutralization data are based on a single experiment (standard in the field), which was conducted with technical quadruplicates. For data normalization, background signals (Fluc signals obtained from cell inoculated with pseudotype particles bearing no S protein) were subtracted from all values and transduction by particles incubated only with medium was set as 0% inhibition. The neutralizing titer 50 (NT50) value, which indicates the plasma/serum dilution that causes a 50% reduction of transduction efficiency, was calculated using a non-linear regression model (inhibitor versus normalized response, variable slope).

Error bars are defined as either standard deviation (SD, ACE2 binding and neutralization data for monoclonal antibodies) or standard error of the mean (SEM, all other data). Data were analyzed using Microsoft Excel (as part of the Microsoft Office software package, version 2019, Microsoft Corporation) and GraphPad Prism 8 version 8.4.3 (GraphPad Software). Statistical significance was tested by two-tailed Student's t test (pseudotype entry, ACE2 binding and cell-cell fusion assays) or Kruskal-Wallis analysis with Dunn's post hoc test (neutralization assays). Only p values of 0.05 or lower were considered statistically significant (p > 0.05, not significant [ns]; $p \leq 0.05$, *; $p \leq 0.01$, **; $p \leq 0.001$, ***). Details on the statistical test and the error bars can be found in the figure legends.